JACS
JOURNAL OF THE AMERICAN CHEMICAL SOCIETY

COMMUNICATION

pubs.acs.org/JACS

Effect of Length and Contact Chemistry on the Electronic Structure and Thermoelectric Properties of Molecular Junctions

Aaron Tan,[†] Janakiraman Balachandran,[‡] Seid Sadat,[‡] Vikram Gavini,[*,‡] Barry D. Dunietz,[*,§] Sung-Yeon Jang,[*,⊥] and Pramod Reddy[*,†,‡]

[†]Department of Materials Science and Engineering, [‡]Department of Mechanical Engineering, and [§]Department of Chemistry, University of Michigan, Ann Arbor, Michigan 48109, United States

[⊥]Department of Chemistry, Kookmin University, Seoul, Korea

Supporting Information

ABSTRACT: We present a combined experimental and computational study that probes the thermoelectric and electrical transport properties of molecular junctions. Experiments were performed on junctions created by trapping aromatic molecules between gold electrodes. The end groups (−SH, −NC) of the aromatic molecules were systematically varied to study the effect of contact coupling strength and contact chemistry. When the coupling of the molecule with one of the electrodes was reduced by switching the terminal chemistry from −SH to −H, the electrical conductance of molecular junctions decreased by an order of magnitude, whereas the thermopower varied by only a few percent. This has been predicted computationally in the past and is experimentally demonstrated for the first time. Further, our experiments and computational modeling indicate the prospect of tuning thermoelectric properties at the molecular scale. In particular, the thiol-terminated aromatic molecular junctions revealed a positive thermopower that increased linearly with length. This positive thermopower is associated with charge transport primarily through the highest occupied molecular orbital, as shown by our computational results. In contrast, a negative thermopower was observed for a corresponding molecular junction terminated by an isocyanide group due to charge transport primarily through the lowest unoccupied molecular orbital.

Novel charge and energy transport phenomena—with important technological applications—are expected to arise in nanometer-sized molecular junctions. Negative differential resistance,[1] rectification,[2] switching,[3] and gating[4] have all been observed in specific molecular junctions and present great potential in advancing electronic applications. In addition to these important molecular−electronic phenomena, recent computational studies[5−8] suggest that it should be possible to create junctions with large thermoelectric efficiencies.

Understanding the structure−property relationship in molecular junctions is a critical step in achieving these important technological goals. It is well known that the chemical structure of molecular junctions plays an important role in determining their transport properties.[9−14] Recently, the dependence of electrical conductance on the structure of molecular junctions has been extensively probed using a variety of experimental techniques.[9,12,13,15] These experiments provide important insights into the dependence of electrical conductance on the molecular backbone, end groups, and metal contacts. However, the relationship between thermoelectric properties and the molecular structure and contact chemistry of junctions has remained relatively unexplored.

In this Communication, we probe the dependence of junction thermoelectric properties on molecular length and contact coupling chemistry using a combined experimental and computational approach. We analyze the electrical conductance and thermopower of a series of molecular junctions using a novel atomic force microscope (AFM)-based technique[16] that enables monolayer measurements not accessible in previous thermopower experiments.[10] In our AFM technique, molecular junctions are created by first self-assembling aromatic molecules into a monolayer on a gold substrate and placing them in contact with a gold-coated AFM tip (Figure 1a). Approximately 100 molecules are trapped by using an AFM tip with a radius of ∼70 nm and by controlling the contact force to be ∼1 nN (more details in the Supporting Information (SI)). Subsequently, known temperature differentials are imposed across the molecular junctions to measure the resulting thermoelectric voltages, from which the thermopower[16] is obtained. Alternately, a voltage differential is applied to obtain the current−voltage ($I-V$) characteristics[17] and the electrical resistance of junctions. The molecules used in this work (Figure 1b) are either singly or doubly terminated with thiol (−SH) or isocyanide (−NC) end groups. Various junctions created from these molecules were probed to study the thermoelectric structure−property relationship of junctions. In addition to the experiments, we computationally model the molecular junctions to obtain insight into the effect of electronic structure on transport properties. In our modeling, the electrical conductance and thermoelectric properties of molecular junctions are obtained by an approach that combines density functional theory (DFT) with a Green's function technique[18−21] implementing the Landauer formalism of transport (see SI for details). A representative model of the junctions used in our calculations is provided in Figure 1c.

Thermoelectric measurements provide additional insights into the electronic structure of molecular junctions that cannot be obtained by electrical transport measurements alone. Specifically, conductance measurements cannot uniquely identify[10,22] whether the highest occupied molecular orbital (HOMO) or the lowest unoccupied molecular orbital (LUMO) lies closer to the Fermi level. However, thermoelectric measurements can answer this question. As will be subsequently discussed in this work, a positive thermopower is

Received: March 9, 2011

dx.doi.org/10.1021/ja202178k | J. Am. Chem. Soc. XXXX, XXX, 000–000

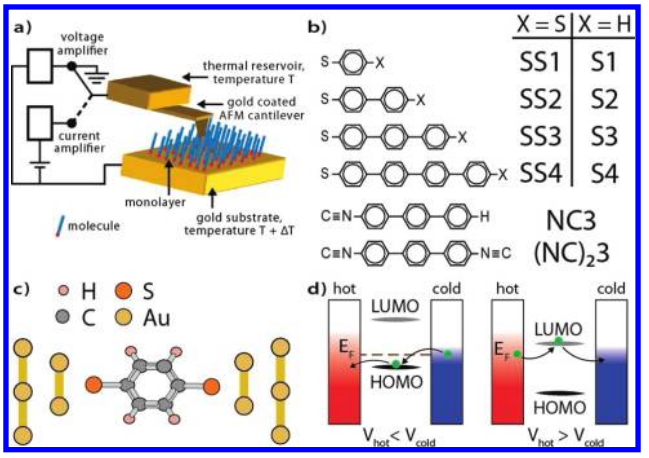

Figure 1. (a) Schematic of the experimental setup for the measurement of the electrical conductance and Seebeck coefficient. (b) Thiol- and isocyanide-terminated aromatic molecules studied in this work. (c) Schematic of the model used for computing the transport properties of the Au−SS1−Au junction. (d) The two scenarios that a Seebeck coefficient measurement can distinguish: HOMO closer to the Fermi level results in a positive Seebeck coefficient, whereas the other scenario results in a negative Seebeck coefficient.

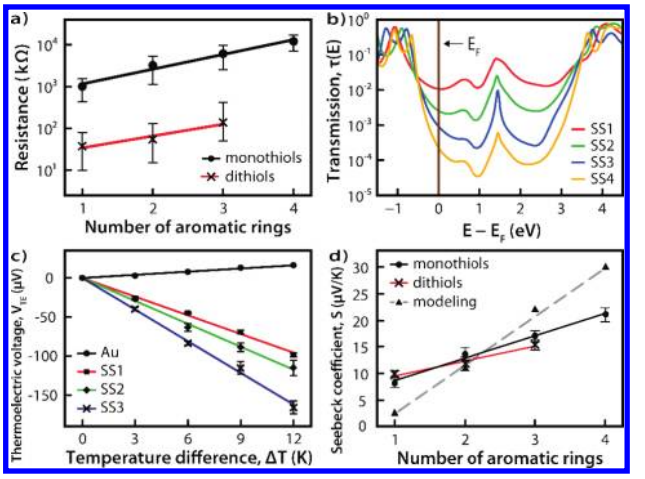

Figure 2. (a) Measured electrical resistances of monothiol and dithiol junctions containing ∼100 molecules. (b) Computed transmission functions for the Au−aromatic dithiol−Au junctions. (c) Thermoelectric voltages obtained for Au−aromatic dithiol−Au junctions, along with those obtained for a Au−Au point contact. (d) Plots of the Seebeck coefficients of the dithiol and monothiol junctions along with the computed values for the Seebeck coefficient of the dithiol junctions.

associated with a HOMO that is closer to the chemical potential, indicating hole-dominated (p-type) transport. In the other scenario, transport is LUMO dominated (n-type) and is related to a negative thermopower. Figure 1d illustrates the two scenarios that thermoelectric measurements can be used to distinguish.

The length dependence of the electrical conductance and Seebeck coefficient of molecular junctions is probed by trapping thiol-terminated aromatic molecules (SS1, SS2, and SS3, shown in Figure 1b) between gold electrodes. The measured resistances of the junctions increase exponentially with the length of the molecules, as shown in Figure 2a. The transport properties of molecular junctions were studied computationally using the Landauer formalism. In this approach, the electrical current (I), the electrical conductance (G), and the thermopower (S) of a molecular junction are[22]

$$I = \frac{2e}{h}\int_{-\infty}^{\infty} \tau(E)[f_1(E) - f_2(E)]\, dE \qquad (1)$$

$$G = \frac{2e^2}{h}\tau(E_F); \quad S = -\frac{\pi^2 k_B{}^2 T}{3|e|}\frac{1}{\tau(E)}\frac{\partial \tau(E)}{\partial E}\bigg|_{E=E_f} \qquad (2)$$

where $\tau(E)$ is the transmission function, $f_1(E)$ and $f_2(E)$ are the Fermi−Dirac distributions corresponding to the electrodes, k_B is the Boltzmann constant, e is the charge of an electron, h is the Planck constant, T is the average absolute temperature of the junction, and E_F is the energy corresponding to the Fermi level of the electrodes. The computed transmission functions, $\tau(E)$, for junctions based on SS1−SS4 molecules are shown in Figure 2b. The transmission at E_F decreases rapidly as the length of the molecules is increased, explaining the observed sharp increase in the resistance of the molecular junctions.

The measured thermoelectric voltages (ΔV) for the thiol-terminated molecular junctions, as a function of the applied temperature differential (ΔT), are shown in Figure 2c. The displayed thermoelectric voltages represent the mean of the measured voltage in 10 independent measurements, where the error bars represent the standard deviation. The magnitude of the measured thermoelectric voltage increases linearly as the applied temperature differential is increased from 0 to 12 K in steps of 3 K. Additional calculations indeed confirm that the measured thermoelectric voltage should increase linearly for the range of applied temperature differentials and are described in the SI. The measured thermoelectric voltage is related to the thermopower of the junction (S) by the following expression:

$$S = S_{Au} - \frac{\Delta V}{\Delta T} \qquad (3)$$

(see the SI for details). Here, S_{Au} is the thermopower of gold, and ΔV is the measured voltage differential between the tip and the grounded substrate. Using this expression and the measured thermoelectric voltages (Figure 2c), the Seebeck coefficients corresponding to junctions based on SS1, SS2, and SS3 molecules are found to be $+9.8 \pm 0.6$, $+11.7 \pm 1.3$, and $+15.4 \pm 1.0\ \mu$V/K, respectively (Table 1). The variation in the measured Seebeck coefficients across experiments arises due to changes in the microscopic details of the metal−molecule contacts.[23] Further, there is a 5% uncertainty in the applied temperature differential,[16] which is also accounted for in the reported standard deviation of the Seebeck coefficients. Control experiments were performed to ensure that the measured thermopower does not arise from Au−Au point contacts. Further details regarding the control experiments are described in the SI and a previous work.[16]

It is insightful to note that, when the intermolecular interactions are weak, the molecules in a multiple molecule junction act as independent channels. In this case, the multiple molecule junction would indeed have a Seebeck coefficient that is invariant with the number of molecules in the junction. The measured multiple molecule junction (monolayer) Seebeck coefficients in this study are in very good agreement with previous measurements of corresponding single-molecule junctions[10] (Table 1). This correlation indicates that the intermolecular interactions in the studied monolayers are small and do not significantly affect the measured Seebeck coefficient.

In our computational studies, the Seebeck coefficients of the molecular junctions are obtained from the transmission function using eq 2. The slope of the transmission function at E_F is negative for all the thiol-terminated junctions. The resulting positive Seebeck coefficients and the corresponding measured values are plotted in Figure 2d. The increase of the Seebeck

dx.doi.org/10.1021/ja202178k | J. Am. Chem. Soc. XXXX, XXX, 000–000

Table 1. Experimental and Computational Values (μV/K) of Seebeck Coefficients for Aromatic Thiol-Based Junctions[a]

	experimentally measured values			
no. of rings	monothiols	dithiols	single-molecule dithiol studies[10]	computed dithiol values
1	8.1 ± 0.8	9.8 ± 0.6	8.7 ± 2.1	2.4
2	13.6 ± 1.2	11.7 ± 1.3	12.9 ± 2.2	10.8
3	17.0 ± 1.0	15.4 ± 1.0	14.2 ± 3.2	21.9
4	21.0 ± 1.3	–	–	29.9

[a] The experimentally measured Seebeck coefficient of the dithiol and monothiol junctions is presented along with the computed Seebeck coefficients of the dithiol junctions. The Seebeck coefficients of single-molecule dithiol junctions obtained in an earlier work are also presented for comparison.

coefficient with the number of rings, as indicated by the measurements, is well reproduced by our computational results and is also consistent with recent computational studies.[24,25] Some of the deviations between experiment and modeling may be due to the microscopic variations in the contact details, which are not addressed by the computational model. Further, molecular vibrations that cause the benzene rings in the molecules to deviate from their equilibrium alignments, which are not considered in this study, also affect transport properties.

Past theoretical studies[22] have elucidated the effect of contact coupling strength on the thermoelectric properties of junctions. These computational studies suggest that when coupling of a molecular junction with one of the electrodes is weakened, the electrical conductance of the junction decreases significantly, whereas the Seebeck coefficient remains relatively invariant. In order to test this hypothesis, we experimentally studied transport properties of junctions fabricated from self-assembled monolayers of monothiol molecules (S1−S4, Figure 1b). The measured electrical resistances of the monothiol molecular junctions are shown in Figure 2a. We estimate that the number of molecules in all junctions is approximately the same, which allows a direct comparison of the junction resistances (see SI for details). These measurements show that the electrical resistance of the monothiol junctions is at least an order of magnitude larger than that of the corresponding dithiol junctions. A similar trend has been observed in previous studies on aliphatic and aromatic molecular junctions.[13,26] We measured the Seebeck coefficients of the monothiol junctions and list them in Table 1. Remarkably, the change in coupling strength has only a marginal effect on the Seebeck coefficient—the difference in the thermopower of monothiol and dithiol junctions is only a few percent and is in strong contrast with the large difference (an order of magnitude) in the electrical resistance of molecular junctions.

This behavior is well explained using a simple model by Paulsson and Datta.[22] In this picture the transmission function of a weakly bound junction is related to the transmission of a strongly bound junction by a scaling factor ($0 < c < 1$):

$$\tau(E)_{\text{weak}} = c\tau(E)_{\text{strong}} \quad (4)$$

In our case, the monothiol and the dithiol junctions represent the weakly and strongly bound junctions, respectively. Considering eqs 2 and 4, it is evident that decreased contact coupling lowers the electrical conductance, whereas the Seebeck coefficient remains invariant to changes in the coupling. Our experimental data provide the first convincing evidence that this simple model[22] can qualitatively capture the effect of weakening the coupling with one of the contacts.

Recent computational[27−29] and experimental work[11,30,31] suggests that end group chemistry provides an attractive route for tuning the electronic energy levels of the junction relative to the chemical potential. Here, we explore the prospect of changing the sign of the Seebeck coefficient by end group chemistry. The positive Seebeck coefficients realized with thiol-terminated junctions suggest p-type transport, which is associated with the HOMO being the closest level to the Fermi energy. Indeed, we confirm this by the calculated transmission, which shows that transport is dominated by the HOMO electronic channel (Figure 2b). A negative sign of the Seebeck coefficient is expected to be realized with the opposite case of LUMO-dominated transport. In fact, it has been hypothesized that n-type transport can be realized with isocynaide end groups.[29] In order to test this hypothesis, we designed experiments where monolayers were created from an isocyanide (−NC)-terminated aromatic molecule (NC3, Figure 1b).

The thermoelectric voltages measured for isocyanide terminated junctions are shown in Figure 3a. The measured thermoelectric voltages indicate a negative Seebeck coefficient of -1.0 ± 0.4 μV/K. The sign of the Seebeck coefficient confirms that transport in the isocyanides is n-type. This result is particularly insightful because previous electrical transport studies[27] of isocyanide junctions were unable to determine whether the HOMO or the LUMO is closer to E_F.

We model the transport properties of the three ringed diisocyanide junctions to analyze the sign dependence of the thermopower on the contact (Figure 3b). For modeling simplicity, we continue to relate the Seebeck coefficient of the mono functionalized molecular junction to a model that involves two end groups, $(NC)_2$3. This modeling scheme is justified by our observation of the invariance of the Seebeck coefficient on the coupling strength. The computed transmission function shows that transport in diisocyanide junctions is dominated by the LUMO channel, resulting in n-type transport. The Seebeck coefficient calculated for the three-ring isocyanide junction ($-1.6\,\mu$V/K) matches in sign with the experiments and has a magnitude comparable to the experimentally measured value of $-1.0 \pm 0.4\,\mu$V/K.

The negative Seebeck coefficient of the isocyanide junction is in contrast to the positive coefficient of the corresponding thiol-terminated junction. We relate the sign reversal to the electronic structure of the junction by observing the electronic density of states (DOS). The electronic DOS in the molecular region for SS3 and $(NC)_2$3 junctions are plotted in Figure 3c. The DOS for the SS3 junction shows that transport is dominated by orbitals below the chemical potential (p-type), resulting in a positive thermopower. In contrast, the electronic DOS of $(NC)_2$3 junctions shows that transport is dominated by orbitals above the chemical potential (n-type), resulting in a negative thermopower. Further details on the orbitals related to the electron transport channels are provided in the SI.

It is interesting to note that when the contact coupling is reduced by removing one of the thiol groups, the Seebeck coefficient is relatively invariant (Table 1). However, changing the end groups from thiol to isocyanide changes not only the magnitude of the Seebeck coefficient but also its sign. This result can be qualitatively understood by noting that when a completely different end group (−NC as opposed to −SH) couples a molecule to an electrode, the electronic structure of the molecular junction is radically changed, as demonstrated by our calculations, resulting in large changes in the Seebeck coefficient. In contrast, when one of the contacts with the electrodes is weakened, we believe that the local DOS in the molecular junction remains qualitatively similar to that of a junction that is strongly bound to both the electrodes, resulting in a relatively invariant Seebeck coefficient. Validating this hypothesis via systematic computational studies is the focus of our future work. We note that the effect of end groups on

dx.doi.org/10.1021/ja202178k |J. Am. Chem. Soc. XXXX, XXX, 000–000

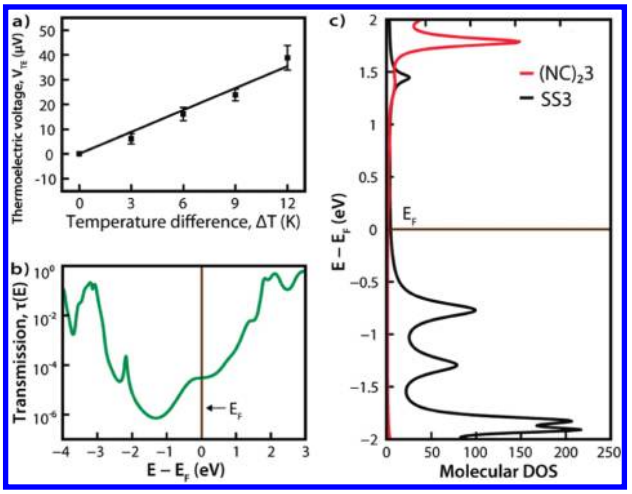

Figure 3. (a) Measured thermoelectric voltages of Au−NC3−Au junctions. (b) Computed transmission functions for the Au−aromatic diisocyanide−Au junction. (c) Molecular electronic density of states around the chemical potential in the SS3 and $(NC)_2$3 junctions.

the sign of the thermopower was also observed in a previous experimental study by one of us in collaboration with others[11] using cyanide (−CN)-terminated molecules. In contrast, the current study of isocyanide (−NC)-terminated junctions not only explores the applicability of another end group to tuning thermoelectric properties but—more importantly—probes the relationship between electronic structure and the sign of thermopower.

To summarize, we have studied thermoelectric properties of molecular junctions via a combined experimental and computational approach. Our studies indicate that the thermopower (Seebeck coefficient) of thiol-terminated junctions is positive in sign and increases with the length of the molecule. Our computational studies associate the positive sign of the junction with the proximity of the HOMO to the chemical potential. We also show that when the coupling of the molecule with one of the electrodes is reduced, the electrical conductance of junctions decreases dramatically, whereas the thermopower remains relatively invariant. Further, we show that for an isocyanide-terminated junction the sign of the thermopower is negative. Our computational studies demonstrate that this change is due to transport being dominated by the LUMO-based channel in the isocyanide junction. These results demonstrate the possibility of tuning the thermoelectric properties of molecular junctions via contact chemistry and molecular structure

■ ASSOCIATED CONTENT

Supporting Information. Computational methodology, experimental procedures, control experiments, and characterization. This material is available free of charge via the Internet at http://pubs.acs.org.

■ AUTHOR INFORMATION

Corresponding Authors

vikramg@umich.edu; bdunietz@umich.edu; syjang@kookmin.ac.kr; pramodr@umich.edu

■ ACKNOWLEDGMENT

A.T. was supported by DOE-BES as part of an EFRC at the University of Michigan (DE-SC0000957). S.S. was supported by the U.S. Department of Energy, Office of Basic Energy Sciences, Division of Materials Sciences and Engineering, under Award DE-SC0004871. B.D.D. gratefully acknowledges support by a DOE-BES award through the Chemical Sciences Geosciences and Biosciences Division (DE-SC0004924), DE-FG02-10ER16174). S.Y.J. thanks financial support by the new faculty research program 2011 of Kookmin University in Korea.

■ REFERENCES

(1) Guisinger, N. P.; Greene, M. E.; Basu, R.; Baluch, A. S.; Hersam, M. C. *Nano Lett.* **2004**, *4*, 55–59.
(2) Chabinyc, M. L.; Chen, X. X.; Holmlin, R. E.; Jacobs, H.; Skulason, H.; Frisbie, C. D.; Mujica, V.; Ratner, M. A.; Rampi, M. A.; Whitesides, G. M. *J. Am. Chem. Soc.* **2002**, *124*, 11730–11736.
(3) Xu, B. Q.; Li, X. L.; Xiao, X. Y.; Sakaguchi, H.; Tao, N. J. *Nano Lett.* **2005**, *5*, 1491–1495.
(4) Song, H.; Kim, Y.; Jang, Y. H.; Jeong, H.; Reed, M. A.; Lee, T. *Nature* **2009**, *462*, 1039–1043.
(5) Bergfield, J. P.; Solis, M. A.; Stafford, C. A. *ACS Nano* **2010**, *4*, 5314–5320.
(6) Bergfield, J. P.; Stafford, C. A. *Nano Lett.* **2009**, *9*, 3072–3076.
(7) Finch, C. M.; Garcia-Suarez, V. M.; Lambert, C. J. *Phys. Rev. B* **2009**, *79*, 033405.
(8) Macia, E. *Phys. Rev. B* **2007**, *75*, 035130.
(9) Xu, B.; Tao, N. *Science* **2003**, *301*, 1221–1223.
(10) Reddy, P.; Jang, S. Y.; Segalman, R. A.; Majumdar, A. *Science* **2007**, *315*, 1568–1571.
(11) Baheti, K.; Malen, J. A.; Doak, P.; Reddy, P.; Jang, S. Y.; Tilley, T. D.; Majumdar, A.; Segalman, R. A. *Nano Lett.* **2008**, *8*, 715–719.
(12) Venkataraman, L.; Klare, J.; Nuckolls, C.; Hybertsen, M.; Steigerwald, M. *Nature* **2006**, *442*, 904–907.
(13) Engelkes, V. B.; Beebe, J. M.; Frisbie, C. D. *J. Am. Chem. Soc.* **2004**, *126*, 14287–14296.
(14) Malen, J. A.; Doak, P.; Baheti, K.; Tilley, T. D.; Segalman, R. A.; Majumdar, A. *Nano Lett.* **2009**, *9*, 1164–1169.
(15) Nitzan, A.; Ratner, M. A. *Science* **2003**, *300*, 1384–1389.
(16) Tan, A.; Sadat, S.; Reddy, P. *Appl. Phys. Lett.* **2010**, *96*, 013110.
(17) Beebe, J. M.; Engelkes, V. B.; Miller, L. L.; Frisbie, C. D. *J. Am. Chem. Soc.* **2002**, *124*, 11268–11269.
(18) Imry, I.; Landauer, R. *Rev. Mod. Phys.* **1999**, *71*, S306.
(19) Prociuk, A.; Van Kuiken, B.; Dunietz, B. D. *J. Chem. Phys.* **2006**, *125*, 204717.
(20) Xue, Y; Datta, S; Ratner, M. A. *Chem. Phys.* **2002**, *281*, 151.
(21) Yaliraki, S. N.; Roitberg, A. E.; Gonzalez, C; Mujica, V; Ratner, M. A. *J. Chem. Phys.* **1999**, *111*, 6997.
(22) Paulsson, M.; Datta, S. *Phys. Rev. B* **2003**, *67*, 241403R.
(23) Malen, J. A.; Doak, P.; Baheti, K.; Tilley, T. D.; Majumdar, A.; Segalman, R. A. *Nano Lett.* **2009**, *9*, 3406–3412.
(24) Ke, S.-H.; Yang, W.; Curtarolo, S.; Baranger, H. U. *Nano Lett.* **2009**, *9*, 1011–1014.
(25) Quek, S. Y.; Choi, H. J.; Louie, S. G.; Neaton, J. B. *ACS Nano* **2011**, *5*, 551–557.
(26) Hong, S.; Reifenberger, R.; Tian, W.; Datta, S.; Henderson, J. I.; Kubiak, C. P. *Superlattices Microstruct.* **2000**, *28*, 289–303.
(27) Ke, S.-H.; Baranger, U. H.; Yang, W. *J. Am. Chem. Soc.* **2004**, *126*, 15897–15904.
(28) Mishchenko, A.; Vonlanthen, D.; Meded, V.; Burkle, M.; Li, C.; Pobelov, I. V.; Bagrets, A.; Viljas, J. K.; Pauly, F.; Evers, F.; Mayor, M.; Wandlowski, T. *Nano Lett.* **2010**, *10*, 156–163.
(29) Xue, Y. Q.; Ratner, M. A. *Phys. Rev. B* **2004**, *69*, 085403.
(30) Zotti, L. A.; Kirchner, T.; Cuevas, J. C.; Pauly, F.; Huhn, T.; Scheer, E.; Erbe, A. *Small* **2010**, *6*, 1529–1535.
(31) Mishchenko, A.; Zotti, L. A.; Vonlanthen, D.; Burkle, M.; Pauly, F.; Cuevas, J. C.; Mayor, M.; Wandlowski, T. *J. Am. Chem. Soc.* **2010**, *133*, 184–187.